

Ph.D. proposal: Mesoscale stratigraphic disturbances in ice sheets relating to plastic anisotropy

Michael Hay, Department of Earth and Space Sciences

February 26, 2015

1 Introduction

Ice cores taken from ice sheets provide an important record of past climate. For accurate interpretation, an ice depth-age relationship is needed. The ice-sheet stratigraphic record is an important tool in constructing this relationship. However, ice-sheet stratigraphy can be disturbed, which can make paleoclimate interpretation difficult. Layers may be overturned, resulting in older ice lying above younger ice. As well, boudinage can occur, potentially removing layers from an ice core record. Especially on the meter or smaller scale, it is likely that a large portion of stratigraphic disruptions are due to the plastic anisotropy of ice.

Individual ice crystals have strong plastic anisotropy, deforming most easily in shear in the basal plane orthogonal to the crystallographic c-axis. Other orientations are around 100 times harder. This can lead to disturbances in several different ways: In both simple shear and vertical uniaxial compression, c-axes tend to cluster near vertical. Vertical maximum fabrics are soft under horizontal simple shear, because the basal planes are aligned with the imposed shear stress. If there is an initial open wrinkle in the stratigraphy, the enhanced simple shear can lead it to overturn into a recumbent fold (Thorsteinsson and Waddington, 2002). Boudinage can occur if there is a harder layer (under extension) surrounded by softer layers. This has likely been observed in electrical conductivity measurements at the WAIS divide core. Also, Alley and others (1997) found “stripes” of non-vertical grains in otherwise vertical-maximum fabric. Similarly, “tilted cone” fabrics can occur, where the maximum of the orientation distribution function is off-vertical (Thorsteinsson and Waddington, 2002). Such fabrics can lead to strain in different components than the applied deviatoric stress. This is a likely mechanism to produce smaller-scale stratigraphic disturbances, even outside of the influence of the bed. Previous work on anisotropic ice flow modeling, such as Gillet-Chaulet and others (2005), has not allowed for general anisotropic viscosity. In addition, it is likely that the coupling of anisotropic flow and fabric evolution is dynamically unstable. For

example, under simple shear, softer-oriented fabrics will evolve towards a softer single maximum faster than initially harder fabrics. This can enhance small initial variations in fabric, and induce the formation of shear bands. In addition, Montgomery-Smith (2011) analytically found that 3-dimensional Stokes flow of a fluid with dense rigid-fiber inclusions, whose orientation distribution function determined by Jeffery’s equation, is unstable. Small nonuniformities in the orientation distribution function can grow quickly, meaning that Jeffery’s equation uncoupled with flow is a poor predictor of fiber orientations. This is mathematically very similar to ice flow with fabric evolution given by Jeffery’s equation (see below).

For my Ph.D., I plan to study the effects of fabric evolution coupled to anisotropic ice flow, which has been a poorly studied area. This research should lead to three or four papers. Our manuscript on the fabric evolution model (see below) is nearing submission. After that, we will do a paper on linear stability of coupled anisotropic flow and fabric evolution. This will then be followed up by work on anisotropic flow laws and a possible numerical model of anisotropic ice-flow.

2 Current work

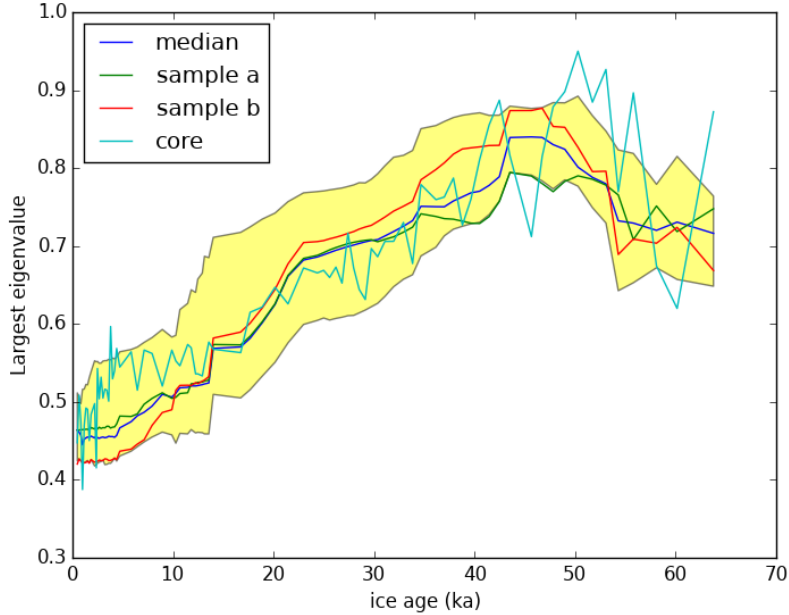
Studying anisotropic ice flow requires a coupled approach between fabric evolution and anisotropic flow. To this end, I have developed an strain-induced ice-fabric evolution model which incorporates a variety of physical processes. We are currently preparing a manuscript based on this model. It treats the fabric as a finite collection of grains, each with properties such as radius, dislocation density, and connectivity between different grains. Unlike previous fabric evolution models, this is mass-conservative. Grains exchange mass through their nearest neighbors, and grains can grow only at the expense of others. Dynamic recrystallization is treated as probabilistic, with the probability depending on temperature and accumulated dislocation density. This is justified because there are unobserved properties which control recrystallization at subgrain scale, such as inclusions and subgrain-scale dislocation density variability. Grain rotation is given by Jeffery’s equation:

$$\dot{c}_i = W_{ij}c_j + \zeta \left(D_{ij}^g c_j + c_i c_j c_k D_{jk}^g \right), \quad (1)$$

where c_i is the unit vector in the direction of the c-axis, D_{ij}^g is the strain rate tensor experienced by the grain, and W_{ij} is the bulk spin tensor. ζ is the softness parameter, which allows for nearest neighbor interaction by effectively transferring stress.

I have forced the model with thin section data from the West Antarctic Ice Sheet (WAIS) divide ice core. Ensemble runs using bootstrapped data show that fabrics which have statistically the same distribution do not converge over time. The strengths of individual fabric realizations can oscillate with respect to other samples. This is seen in the figure with the largest eigenvalue of the fabrics.

Figure 1: Modeled versus thin-section data from the WAIS divide core. The shaded area is the 90% confidence interval and median of evolution of the distribution of the fabric sample at the top of the core, inferred from repeated bootstrap samples of the thin-section data. Two sample realizations and the median are also included.



This occurs even if there is no recrystallization, and is likely due to the effects of grain connectivity. These differences are related to sample size. However, several hundred grains can occupy a large volume. Despite two samples being taken from the same distribution, the response to applied stress can nonetheless vary greatly. Thus, fabric variability could be an important driver behind flow disturbances.

3 Research plan

We will be submitting the manuscript on the fabric model shortly. After that, I have partially developed an analytical first-order perturbation model of coupled anisotropic ice flow and fabric evolution that will allow us to look at the stability of anisotropic flow (see the next section). This will lead to a second paper for submission in 2015.

3.1 Stability of anisotropic flow

The General Orthotropic Linear Flow law (GOLF) of Gillet-Chaulet and others (2005) is an analytically more tractable model for orthotropic flow. The fabric is assumed to possess three axes of symmetry, and can be described completely by its second-order orientation tensor. In a similar manner to Montgomery-Smith (2011), I plan to investigate the stability of orthotropic flow coupled to a fabric evolution model using linear stability analysis.

Fabric evolution is modeled using a form of the Jeffery's equation for orthotropic orientation distribution functions (Gillet-Chaulet and others, 2006),

$$\frac{\partial A_{ij}}{\partial t} = -\frac{\partial}{\partial x_k} A_{ij} u_k + W_{ik} A_{kj} - A_{ik} W_{kj} - (D_{ik} W_{kj} + D_{kj} W_{ik}) + 2\mathbb{A}_{ijkl} C_{kl} \quad (2)$$

Jeffery's equation for an orientation tensor of order n depends on the orientation tensor of order $n+2$, here the fourth-order orientation tensor \mathbb{A}_{ijkl} . Therefore, a closure approximations for \mathbb{A}_{ijkl} is required. In the literature, various approximations are used. Gillet-Chaulet and others (2006) used the "invariant-based optimal fitting closure approximation" which is fitted based on 63 parameters. Instead, we use the quadratic closure, in which $\mathbb{A}_{ijkl} = A_{ij} A_{kl}$. This is simple, and is exact for fabrics whose c-axes are concentrated in a single orientation.

The constitutive relation in tensor form is given by,

$$S_{ij} = \eta_0 \left[\eta_r M_{rkl} D_{kl} (M_{rij}^D) + \eta_{r+3} (D_{ik} M_{rkj} + D_{kj} M_{rik})^D \right], \quad (3)$$

where S_{ij} is the deviatoric stress tensor, and \dot{D}_{ij} is the strain rate tensor. $M_{rij} = v_{ri} v_{rj}$ (no sum in r), where v_{ri} is the r^{th} eigenvector of the second order orientation tensor A_{ij} . η_r are six independent flow parameters, depending on A_{ij} and the chosen homogenization model to transfer between the stress and strain experienced by an individual grain to that experienced by the polycrystal. Here, I assume homogeneous strain. Then, we can assume that basal glide is solely responsible for deformation, leading to the following relation between macroscopic stress and macroscopic strain rate. This leads to the inverse form of GOLF, which is a linear relationship given by,

$$D_{ij} = \frac{1}{2\eta} [-2\mathbb{A}_{ijkl} S_{kl} S_{ik} A_{kj} + A_{ik} S_{kj}] = H_{ijkl} S_{kl}, \quad (4)$$

We assume, for the unperturbed equations, that we are working in the orthotropic reference frame. Then, A_{ij} become diagonal tensors of the fabric eigenvalues. Also, M_{ij} reduces to δ_{ij} . This simplifies equation (3) to

$$S_{ij} = \eta_0 [\eta_r D_{ik} \delta_{ij} + 2\eta D_{ij} + \lambda_r D_{kk} \delta_{ij}] = L_{ijkl} D_{kl}. \quad (5)$$

We can then substitute equation 3 into equation 4. Due to the linearity, this can be written by composing the linear operators to get,

$$D_{ij} = H_{ijkl} L_{klmn} D_{mn} \quad (6)$$

The η_i are properly fitted if the equation is satisfied for arbitrary D_{ij} . Therefore, the composition has to yield the identity fourth order tensor. Note that $H_{ijkl} = H_{ijlk} = H_{jilk}$, and likewise for L_{ijkl} . Therefore, we can write this system in Voigt notation as,

$$\underline{\mathbf{d}} = \underline{\mathbf{H}} \cdot \underline{\mathbf{L}} \cdot \underline{\mathbf{d}}, \quad (7)$$

where $\underline{\mathbf{H}}$ and $\underline{\mathbf{L}}$ are 6×6 matrices, and $d = [D_{11}, D_{22}, D_{33}, D_{32}, D_{23}, D_{21}]$. Now, in the orthotropic reference frame, it can be seen that both H and L are “kite” matrices. They have possible nonzero entries in the 3×3 submatrix in the upper left, and nonzeros on the diagonal. $\underline{\mathbf{L}}$ is derived in Gillet-Chaulet and others (2005). They are nonunique because both S_{ij} and D_{ij} have zero trace.

$\underline{\mathbf{H}}$ is determined by the fabric eigenvalues, while $\underline{\mathbf{H}}$ is a function of the η_r . Thus, we need to choose η_r such that tensors with zero trace are unchanged by the transformation. $\underline{\mathbf{H}}$ has three linearly independent components, and twelve nonzero components. $\underline{\mathbf{H}}^{-1}$ has 6 unique components. In the “kite” portion, the three nonzero components of each row are identical. The “tail” of the kite is trivial to invert, with,

$$\eta_{3+i} = \frac{1}{a_j + a_k}, \quad (8)$$

for $i = 1, 2, 3$ and $i \neq j, k$. Then, the remaining three η_i can be found by,

$$\eta_1 + 4\eta_4 = -\eta_2 + 2\eta_5 = -\eta_3 + 2\eta_6 = \text{const} \quad (9)$$

Note that we can chose the three λ_i such that $\underline{\mathbf{H}}^{-1} = \underline{\mathbf{L}}$, thus this choice of η_i exactly fits the flow law to the homogeneous stress homogenization scheme.

To study the stability of GOLF flow in response to perturbations, I plan to do stability analysis in response to perturbations of the ODF. We assume that there is fluid obeying the GOLF flow law filling all of \mathbb{R}^3 with an unperturbed velocity gradient \bar{U}_{ij} . Now, we introduce a perturbation at time $t = 0$ of a specific wavenumber κ to A_{ij} :

$$A_{ij} \rightarrow \bar{A}_{ij} + \epsilon \hat{A}_{ij} e^{i\kappa_k x_k} \quad (10)$$

Now, in response to this initial perturbation, the quantities depending on A_{ij} are perturbed by the same wavenumber:

1. $u_j \rightarrow \bar{u}_j + \epsilon \hat{u}_j e^{i\kappa_k x_k}$
2. $p \rightarrow \bar{p} + \epsilon \hat{p} e^{i\kappa_k x_k}$
3. $S_{ij} \rightarrow \bar{S}_{ij} + \epsilon \hat{S}_{ij} e^{i\kappa_k x_k}$
4. $\phi \rightarrow \bar{\phi} + \epsilon \hat{\phi} e^{i\kappa_k x_k}$
5. $\mathbb{A}_{ijkl} \rightarrow \bar{\mathbb{A}}_{ijkl} + \epsilon \hat{\mathbb{A}}_{ijkl}$

These are valid due to linearity. The “hat” quantities are assumed to be constant over space, but may vary with time. First, to satisfy Jeffery’s equation, it can be shown that at time t , $\kappa_j(t) = e^{-tU_{kj}}\kappa_k^0$, where κ_k^0 is the initial wavenumber at $t = 0$ (Montgomery-Smith, 2011). Compressibility and force balance require

$$\frac{\partial}{\partial x_j}(\hat{u}_j e^{i\kappa_k x_k}) = 0 \quad (11)$$

$$\frac{\partial}{\partial x_j}(\hat{S}_{ij} - \hat{p})e^{i\kappa_k x_k} = 0 \quad (12)$$

Since \hat{S}_{ij} , \hat{p} , and \hat{u}_i are spatially homogeneous, these reduce to $\kappa_k u_k = 0$ and $\kappa_k \sigma_{jk} - \kappa_j \hat{p} = 0$, respectively. The expression for \hat{S}_{ij} is found by substituting the perturbed quantities into equation and discarding terms of ϵ^2 and higher. Zero-order terms vanish, as they satisfy the original equations. M_{rij} is the product $v_{ri}v_{rj}$, respectively, of the perturbed A_{ij} . The perturbed eigenvalues and eigenvectors themselves can be assumed to be linear perturbations depending on the perturbed A_{ij} . Therefore, the first-order perturbed Stokes equations reduce to a set of four homogeneous linear algebraic equations depending on \hat{A}_{ij} and \hat{u}_k .

Now we look for the equation for the time evolution of the perturbation \hat{A}_{ij} . This is done by putting the perturbed quantities W_{ij} , D_{ij} , A_{ij} , \mathbb{A}_{ijkl} , dividing out the exponential, and discarding higher-order terms. This yields,

$$\begin{aligned} \frac{\partial \hat{A}_{ij}}{\partial t} = & -\frac{\partial}{\partial x_k} \left(\hat{A}_{ij} \bar{U}_k + \bar{A}_{ij} \hat{u}_k \right) + \bar{W}_{ik} \hat{A}_{kj} + \hat{W}_{ik} \bar{A}_{kj} - \bar{A}_{ik} \hat{W}_{kj} \\ & - \hat{A}_{ik} \bar{W}_{kj} - \hat{D}_{ik} \bar{W}_{kj} - \bar{D}_{ik} \hat{W}_{kj} \\ & - \hat{D}_{kj} \bar{W}_{ik} - \bar{D}_{kj} \hat{W}_{ik} + 2(\bar{\mathbb{A}}_{ijkl} \hat{D}_{kl} + \hat{\mathbb{A}}_{ijkl} \bar{D}_{kl}) \end{aligned} \quad (13)$$

Like the perturbed Stokes equations, the exponential is the only spatially nonhomogeneous component of each equation. Therefore, the perturbed Jefferys equation becomes an ordinary differential equation for six independent components of \hat{A}_{ij} . Alternatively, the perturbed quantities can be perturbations of the three eigenvalues, combined with a small rotation of the axes of orthotropic symmetry. In that case, the perturbation of η_{i+3} for $i = 1, 2, 3$ is $\hat{\eta}_{i+3} = 1 - \hat{a}_j + \hat{a}_k$, $j, k \neq i$. The other η follow. The perturbation of the reference frame takes the form of a skew symmetric matrix whose entries are the three Euler angles of rotation. By examining the eigenvalues of the resulting system matrix, we can examine stability as a function of wavenumber, initial fabric and flow. This will let us look at the linear stability of anisotropic flow in a range of situations, such as tilted cones fabric in pure shear, or horizontally varying fabric in simple shear. This analytical treatment of stability will provide information on both where instabilities can occur, and over which length scales.

3.2 Constitutive relations for anisotropic flow

There has not been a tremendous amount of work on anisotropic constitutive relations. GOLF is the only example used in flow calculations that goes beyond using an enhancement factor, or very simple treatments of anisotropy. The GOLF flow law conveniently describes many aspects of anisotropic flow. I think a paper to study the strengths and shortcomings of GOLF could be useful. GOLF assumes that the fabric orientation distribution function does not have moments above fourth order, and further, the fourth order orientation tensor depends completely upon the second-order tensor due to the closure approximation. It assumes orthotropy, which is not satisfied for general fourth-order orientation tensors. For linear flow of a material with transversely orthotropic components, the viscosity tensor does not depend on orientation tensors higher than fourth order (Advani and Tucker III, 1987). Thus, we have the following questions regarding the accuracy of the ODF approximation in GOLF:

1. Are non-orthotropic components of the fourth-order orientation tensor important? Non-orthotropic fabrics, such as multiple-maxima fabrics, are observed relatively commonly. Does this have a major effect on flow?
2. Would the inclusion of higher-order terms in the fabric development equation affect the evolution of the second and fourth-order orientation tensors? While these higher order terms do not affect linear flow, they do affect fabric development.

To answer the first question, we can generate non-orthotropic fourth-order tensors from fabric samples, and see how this differs from the orthotropic approximation. For the second question, we can compare a higher-order closure approximation of Jeffery's equation (e.g. Montgomery-Smith and others (2010)). It is also possible to extend the first-order model of the previous section to include higher-order orientation tensors.

If interaction between grains is important, then the flow depends on higher-order orientation tensors of the ODF. As part of the current fabric model, stress on individual grains is calculated from bulk strain. For the resulting strain on individual grains to be consistent with bulk strain with nearest-neighbor interaction, the model uses fixed-point iteration to adjust the softness parameter of each grain until convergence with bulk strain is achieved. Numerical results from this indicate that while nearest-neighbor interaction is important for fabric development, it only has a small effect on bulk viscosity. The change in the stress tensor before and after this procedure are on the order of 1%. It is possible to find pathological fabrics where this is not the case, but grain interactions appear to only have a minor effect on bulk flow. I can study this more by using parts of my current fabric model to see what, if any, realistic situations where interaction is significant.

From Azuma (1994), strain on an individual grain is proportional to approximately the third power of resolved shear stress on the basal plane. In existing anisotropic flow laws such as GOLF, the anisotropy is accounted for by a tensor

viscosity, and thus the flow law can only represent anisotropy by a linear factor. The nonlinear part of viscosity is scalar, which causes strain on hard grains to be overestimated. Like grain interaction, this may not be a significant effect for realistic fabrics. However, to my knowledge, this has not been studied for ice. I will be able to look at this numerically using a modification of a portion of my current fabric model. By studying these issues, we will be able to see if GOLF is good enough for any realistic flow situations, or if a more general constitutive relation would be useful. Furthermore, we can also compare other anisotropic constitutive relations such as the CAFFE model (Placidi and others, 2010).

3.3 Numerical ice flow model

To take things beyond first order perturbations, the analytical work will be followed up a numerical ice-flow model to look at smaller-scale flow. We may adapt the existing Elmer/Ice model using the GOLF flow law to meter-scale flow. Alternatively, if we decide on a different flow law, a simple finite-volume scheme could be used since we will be working in a box geometry. A conservative upwind scheme could be used for fabric development. The numerical model will allow us to study the progression of boudinage and layer folding, as well as the effects of tilted-cone fabrics and stripes.

4 Funding

This research is currently funded by NSF Grant 0636996 for the study of anisotropic ice flow. This will continue until June 2016, although an extension is likely. If funding is needed beyond then, we will seek another grant or rely on TA funding.

References

- Advani, Suresh G and Charles L Tucker III, 1987. The use of tensors to describe and predict fiber orientation in short fiber composites, *Journal of Rheology (1978-present)*, **31**(8), 751–784.
- Alley, RB, AJ Gow, DA Meese, JJ Fitzpatrick, ED Waddington and JF Bolzan, 1997. Grain-scale processes, folding, and stratigraphic disturbance in the GISP2 ice core, *Journal of Geophysical Research*, **102**(C12), 26819–26.
- Azuma, N., 1994. A flow law for anisotropic ice and its application to ice sheets, *Earth and Planetary Science Letters*, **128**(3-4), 601–614.
- Gillet-Chaulet, Fabien, Olivier Gagliardini, Jacques Meyssonier, Maurine Montagnat and Olivier Castelnau, 2005. A user-friendly anisotropic flow law for ice-sheet modelling, *Journal of glaciology*, **51**(172), 3–14.

- Gillet-Chaulet, F., O. Gagliardini, J. Meyssonier, T. Zwinger and J. Ruokola, 2006. Flow-induced anisotropy in polar ice and related ice-sheet flow modelling, *Journal of Non-Newtonian Fluid Mechanics*, **134**(1), 33–43.
- Montgomery-Smith, Stephen, 2011. Perturbations of the coupled Jeffery-Stokes equations, *Journal of Fluid Mechanics*, **681**, 622–638.
- Montgomery-Smith, Stephen, David A Jack and Douglas E Smith, 2010. A systematic approach to obtaining numerical solutions of Jefferys type equations using spherical harmonics, *Composites Part A: Applied Science and Manufacturing*, **41**(7), 827–835.
- Placidi, Luca, Ralf Greve, Hakime Seddik and Sérgio H Faria, 2010. Continuum-mechanical, Anisotropic Flow model for polar ice masses, based on an anisotropic Flow Enhancement factor, *Continuum Mechanics and Thermodynamics*, **22**(3), 221–237.
- Thorsteinsson, T. and E.D. Waddington, 2002. Folding in strongly anisotropic layers near ice-sheet centers, *Annals of Glaciology*, **35**(1), 480–486.